

Article

Observation and Simulation of CO₂ Fluxes in Rice Paddy Ecosystems Based on the Eddy Covariance Technique

Jinghan Wang¹, Jiayan Wang¹, Hui Zhao^{1,2,*}  and Youfei Zheng³

¹ School of Resources and Environmental Engineering, Jiangsu University of Technology, Changzhou 213001, China; 2022361210@smail.jsut.edu.cn (J.W.); 2023361212@smail.jsut.edu.cn (J.W.)

² Department of Environmental Science and Engineering, Fudan University, Shanghai 200438, China

³ Collaborative Innovation Center of Atmospheric Environment and Equipment Technology, Jiangsu Key Laboratory of Atmospheric Environment Monitoring and Pollution Control (AEMPC), Nanjing University of Information Science & Technology, Nanjing 210044, China; zhengyf@nuist.edu.cn

* Correspondence: zhaohui_nuist@163.com; Tel.: +86-156-0158-5660

Abstract: As constituents of one of the vital agricultural ecosystems, paddy fields exert significant influence on the global carbon cycle. Therefore, conducting observations and simulations of CO₂ flux in rice paddy is of significant importance for gaining deeper insights into the functionality of agricultural ecosystems. This study utilized an eddy covariance system to observe and analyze the CO₂ flux in a rice paddy field in Eastern China and also introduced and parameterized the Jarvis multiplicative model to predict the CO₂ flux. Results indicate that throughout the observation period, the range of CO₂ flux in the paddy field was -0.1 to $-38.4 \mu\text{mol}/(\text{m}^2\cdot\text{s})$, with a mean of $-12.9 \mu\text{mol}/(\text{m}^2\cdot\text{s})$. The highest CO₂ flux occurred during the rice flowering period with peak photosynthetic activity and maximum CO₂ absorption. Diurnal variation in CO₂ flux exhibited a “U”-shaped curve, with flux reaching its peak absorption at 11:30. The CO₂ flux was notably higher in the morning than in the afternoon. The nocturnal CO₂ flux remained relatively stable, primarily originating from respiratory CO₂ emissions. The rice canopy CO₂ flux model was revised using boundary line analysis, elucidating that photosynthetically active radiation, temperature, vapor pressure deficit, phenological stage, time, and concentration are pivotal factors influencing CO₂ flux. The simulation of CO₂ flux using the parameterized model, compared with measured values, reveals the efficacy of the established parameter model in simulating rice CO₂ flux. This study holds significant importance in comprehending the carbon cycling process within paddy ecosystems, furnishing scientific grounds for future climate change and environmental management endeavors.

Keywords: CO₂ flux model; eddy covariance technique; CO₂ concentration; photosynthetically active radiation; vapor pressure deficit



Citation: Wang, J.; Wang, J.; Zhao, H.; Zheng, Y. Observation and Simulation of CO₂ Fluxes in Rice Paddy Ecosystems Based on the Eddy Covariance Technique. *Atmosphere* **2024**, *15*, 517. <https://doi.org/10.3390/atmos15050517>

Academic Editor: Rapsomanikis Spyridon

Received: 2 April 2024

Revised: 21 April 2024

Accepted: 23 April 2024

Published: 24 April 2024



Copyright: © 2024 by the authors. Licensee MDPI, Basel, Switzerland. This article is an open access article distributed under the terms and conditions of the Creative Commons Attribution (CC BY) license (<https://creativecommons.org/licenses/by/4.0/>).

1. Introduction

The Intergovernmental Panel on Climate Change (IPCC) Fifth Assessment Report unequivocally states that global climate warming is an indisputable fact. The primary cause of global warming is the continuous increase in the emissions of greenhouse gases such as carbon dioxide (CO₂), methane (CH₄), nitrous oxide (N₂O), and water vapor in the atmosphere. This leads to an excessive absorption of solar radiation and other energy reflected from the Earth’s surface by the atmosphere, resulting in the greenhouse effect and ultimately causing gradual global warming [1]. Since the Industrial Revolution, with the development of social productivity and the expansion of economic scale, human emissions of greenhouse gases, primarily CO₂, have increased sharply. Currently, excessive CO₂ emissions are considered the primary cause of anthropogenic influence on the greenhouse effect. Studies have shown that the global atmospheric CO₂ concentration has risen from 315 ppm in the mid-20th century to the current 368 ppm, with emissions from fossil fuel combustion accounting for 57% of total greenhouse gas emissions [2].

Constituting one of the four major carbon reservoirs globally, terrestrial ecosystems serve as a bridge for CO₂ exchange between the atmosphere and the biosphere. They not only utilize vegetation photosynthesis to absorb and store CO₂ from the atmosphere, acting as carbon sinks, but also release CO₂ into the atmosphere through vegetation and soil respiration, serving as stable carbon sources [3]. It is this unique dual nature of terrestrial ecosystems that gives them a pivotal role in the global carbon balance. Terrestrial ecosystems are primarily composed of forest ecosystems, grassland ecosystems, and agricultural ecosystems. Compared to the other two land covers, agricultural ecosystems are more susceptible to human production activities, thus exhibiting more variability in CO₂ exchange and warranting further research [4]. Furthermore, research on CO₂ fluxes both domestically and internationally has predominantly focused on forests and grasslands, leaving relatively little attention to agricultural ecosystems [5]. Therefore, studying the carbon fluxes in agricultural ecosystems is of significant importance for a deeper understanding of the carbon cycling patterns within terrestrial ecosystems and for predicting future global changes.

Currently, there are mainly two methods for observing CO₂ flux: the chamber method and micrometeorological methods [6]. Among them, the chamber method, due to its simplicity and low cost, has been widely used, and most domestic studies are based on this method [7]. When using this method for measurement, the chamber needs to be closed, which changes the growth environment of the crop to some extent, thus affecting the accuracy of the experimental results [7]. The gradient method and the eddy covariance method are two commonly used micrometeorological methods for observing CO₂ flux in ecosystems. When using the gradient method to measure atmospheric CO₂ flux, observations of CO₂ concentration, wind speed, temperature, humidity, etc. need to be made at different heights above the crop canopy to calculate CO₂ flux [8]. This method requires high requirements for gas analyzers and sampling systems and suitable meteorological conditions during observations [8,9]. The micrometeorological method based on the eddy covariance technique is an advanced method developed in recent years for measuring atmospheric fluxes in ecosystems. This method is still relatively scarce in the observation of CO₂ and water vapor fluxes; thus, further research is necessary [10]. On the other hand, previous studies on CO₂ flux have mainly focused on field observations. Given the complex factors affecting CO₂ flux and the limited efficacy of single-factor analysis, it is necessary to integrate multiple influencing factors and establish suitable models for predicting CO₂ flux.

Based on the concerns mentioned above, the present study employed an eddy covariance system to continuously observe the CO₂ flux within the rice canopy and analyze its variation characteristics. Furthermore, the study introduced and parameterized a canopy CO₂ flux model to predict CO₂ flux, thereby providing important foundations for the accurate assessment of ecosystem carbon fluxes in China and the formulation of strategies for sustainable agricultural development. This research aims to offer scientific support for the formulation of relevant policies and the sustainable development of agricultural production.

2. Materials and Methods

2.1. Site Description

The observation site is located in the rice paddies of the Yongfeng Agricultural Meteorological Station at Nanjing University of Information Science and Technology (32°21' N, 118°69' E, elevation: approximately 22 m). The observation period for CO₂ flux in the rice paddies was from 15 July 2017 to 8 October 2017. The site covers an area that is approximately 250 m in length and 150 m in width, with an open and flat terrain and no tall buildings obstructing the surrounding area [11]. The soil type at the site is primarily yellow–brown soil, with a pH value of approximately 7.0. The soil organic matter content is 12.8 g·kg⁻¹, total nitrogen content is 0.82 g·kg⁻¹, available phosphorus content is 4.4 mg·kg⁻¹, and available potassium content is 52.1 g·kg⁻¹.

2.2. Observation Instruments

The CO₂ flux observation instrument used in this study is an open-path eddy covariance system. Based on the eddy covariance principle, it utilizes fast-response sensors to measure the exchange of substances and energy between the atmosphere and the underlying surface. This method is considered the best approach for measuring carbon and water exchange fluxes in terrestrial ecosystems in recent years and has become the main technology of international flux observation networks. The eddy covariance system mainly consists of a CSAT3 three-dimensional sonic anemometer (Campbell Scientific Inc., Logan, UT, USA) and an LI-7500 H₂O/CO₂ infrared gas analyzer (LI-COR Biosciences, Lincoln, NE, USA), used to observe three-dimensional wind speed, sonic temperature, CO₂, water vapor concentration, etc. The original data are sampled at a frequency of 10 Hz and recorded and processed online by the CR3000 data logger, and 30 min flux values and other parameters are stored in the data logger.

It should be noted that the CO₂ uptake fluxes discussed in this study represent the daytime net ecosystem carbon exchange (NEE), namely the net CO₂ uptake by rice, denoted as follows:

$$F_{\text{CO}_2} = F_{\text{C}} + F_{\text{st}} \quad (1)$$

$$F_{\text{st}} = h\Delta c/\Delta t \quad (2)$$

Here, F_{C} represents the CO₂ turbulent flux, which can be directly obtained through the eddy covariance system; F_{st} represents the atmospheric CO₂ storage flux below the instrument height; h is the height of the eddy covariance system; and Δc represents the change in CO₂ concentration over the time interval Δt .

2.3. Data Processing

The raw data obtained through the eddy covariance system have a sampling frequency of 10 Hz. The 30 min flux calculations and preprocessing were performed using the EddyPro (v6.2.2, LI-COR Inc., Lincoln, NE, USA) software. This software is highly versatile and has been widely used for calculating fluxes of CO₂, H₂O, CH₄, and other trace gases and energy. The preprocessing steps include outlier removal, time delay correction, secondary coordinate axis rotation, frequency response correction, and water vapor density correction among others [12]. To ensure data accuracy, the 30 min flux data outputted by the software require further quality control, as described below.

Firstly, data with negative values occurring during nighttime (when total solar radiation < 10 W·m⁻²) are removed. Secondly, outlier data that significantly deviate from the normal range of data variation are eliminated. Since precipitation can disrupt the normal atmospheric flow in agricultural ecosystems and may even lead to instrument malfunction, data collected during rainy periods are also excluded [11]. Finally, flux data corresponding to friction wind speeds less than 0.15 m·s⁻¹ are removed to eliminate the influence of insufficiently developed turbulence [12].

Throughout the entire observation period, adverse weather conditions, instrument failures, power outages, and other factors may lead to a significant number of missing data. Therefore, it is necessary to interpolate the missing data mentioned above. The interpolation methods mainly include the following: for <3 h of continuous missing data, simple linear interpolation is applied [9]; for >3 h and <1 day of continuous missing data, the daily average change method is used [13]. In addition, continuous missing data lasting >1 day are not interpolated and are considered invalid data.

2.4. CO₂ Flux Model

Based on the study by Tong et al. [14], the Jarvis stomatal conductance multiplicative model for rice leaves is extended to simulate the CO₂ flux within the rice canopy. The specific expression of this model is as follows:

$$F'_{\text{CO}_2} = F_{\text{max,CO}_2} \times \max[f_{\text{min}}, (f_{\text{temp}}f_{\text{VPD}})] \times f_{\text{PAR}} \times f_{\text{Phen}} \times f_{\text{Time}} \times f_{\text{CO}_2} \quad (3)$$

Here, F'_{CO_2} represents the CO₂ absorption flux of rice and F_{max,CO_2} is the maximum CO₂ absorption flux. f_{min} is the ratio of minimum CO₂ flux to maximum CO₂ flux. f_{temp} , f_{VPD} , f_{PAR} , f_{phen} , f_{Time} , and f_{CO_2} represent the stress coefficients of temperature (T), vapor pressure deficit (VPD), photosynthetically active radiation (PAR), phenology (Phen), time (Time), and CO₂ concentration to the maximum canopy CO₂ flux, respectively [14]. These values are all within the range of 0 to 1. The parameters of each stress coefficient are obtained through the boundary line analysis technique of quantile regression [15]. Specifically, scatter plots are made with each climatic environmental variable as the horizontal axis and relative canopy CO₂ flux as the vertical axis. Using the form of stress coefficients provided in the literature, the peripheral data points are fitted, thus obtaining the specific expressions of stress coefficients suitable for the rice CO₂ flux model in the local area.

(1) Temperature stress coefficient (f_{temp})

$$f_{temp} = \begin{cases} \left(\frac{T - T_{min}}{T_{opt} - T_{min}} \right) \times \left(\frac{T_{max} - T}{T_{max} - T_{opt}} \right)^{bt}, & \text{if } T_{min} < T < T_{max} \\ f_{min}, & \text{if } T \geq T_{max} \text{ or } T \leq T_{min} \end{cases} \quad (4)$$

Here, T represents the hourly average temperature (°C), T_{max} and T_{min} denote the maximum and minimum temperatures at which the CO₂ flux reaches its minimum value f_{min} , and T_{opt} represents the temperature at which the CO₂ flux is maximum, also known as the optimum temperature. The calculation of the bt value is as follows:

$$bt = \frac{T_{max} - T_{opt}}{T_{opt} - T_{min}} \quad (5)$$

(2) Vapor pressure deficit stress coefficient (f_{VPD})

$$f_{VPD} = \min \left\{ 1, \max \left\{ f_{min}, \frac{(1 - f_{min}) \times (VPD_{min} - VPD)}{VPD_{min} - VPD_{max}} + f_{min} \right\} \right\} \quad (6)$$

Here, VPD represents the hourly vapor pressure deficit (kPa), VPD_{max} is the VPD value at which the CO₂ flux begins to be limited, and VPD_{min} is the VPD value at which the CO₂ flux is restricted to reach f_{min} .

(3) Photosynthetically active radiation stress coefficient (f_{PAR})

$$f_{PAR} = 1 - e^{(-a \times PAR)} \quad (7)$$

Here, PAR represents the photosynthetically active radiation, and a is a constant representing the parameter obtained from fitting the light response curve.

(4) Phenology stress coefficient (f_{phen})

$$f_{phen} = \begin{cases} c_1 DAY + d_1, & \text{if } Day < Day_c \\ c_2 DAY + d_2, & \text{if } Day > Day_c \end{cases} \quad (8)$$

Here, Day represents the number of days since rice sowing, and Day_c represents the number of days after sowing when the relative CO₂ flux reaches its maximum value.

(5) Time stress coefficient (f_{Time})

$$f_{Time} = \frac{1}{\left(1 + \left(\frac{Time}{e} \right)^f \right)} \quad (9)$$

Here, Time represents a specific moment of the day, and e and f are parameters obtained after fitting.

(6) CO₂ concentration stress coefficient (f_{CO_2})

$$f_{\text{CO}_2} = \min \left\{ 1, \max \left\{ f_{\min}, \frac{(1 - f_{\min}) \times (C_{\text{CO}_2, \min} - C_{\text{CO}_2})}{C_{\text{CO}_2, \min} - C_{\text{CO}_2, \max}} + f_{\min} \right\} \right\} \quad (10)$$

Here, C_{CO_2} represents the hourly CO_2 concentration, $C_{\text{CO}_2, \min}$ is the CO_2 concentration at which the relative CO_2 flux reaches f_{\min} , and $C_{\text{CO}_2, \max}$ is the CO_2 concentration at which the relative CO_2 absorption flux reaches its maximum value.

3. Results and Discussion

3.1. Variations in Meteorological Factors and CO_2 Concentration

Figure 1 illustrates the daily variations in meteorological factors such as T, relative humidity (RH), PAR, and VPD during the rice growing season. It can be observed that the daily average ranges of T, RH, PAR, and VPD during the rice growing season are 14.1~34.7 °C, 49.1~84.8%, 128~786 $\mu\text{mol}\cdot(\text{m}^2\cdot\text{s})^{-1}$, and 0.25~2.81 KPa, respectively, with means of 26.1 °C, 69.9%, 387.9 $\mu\text{mol}\cdot(\text{m}^2\cdot\text{s})^{-1}$, and 1.10 KPa.

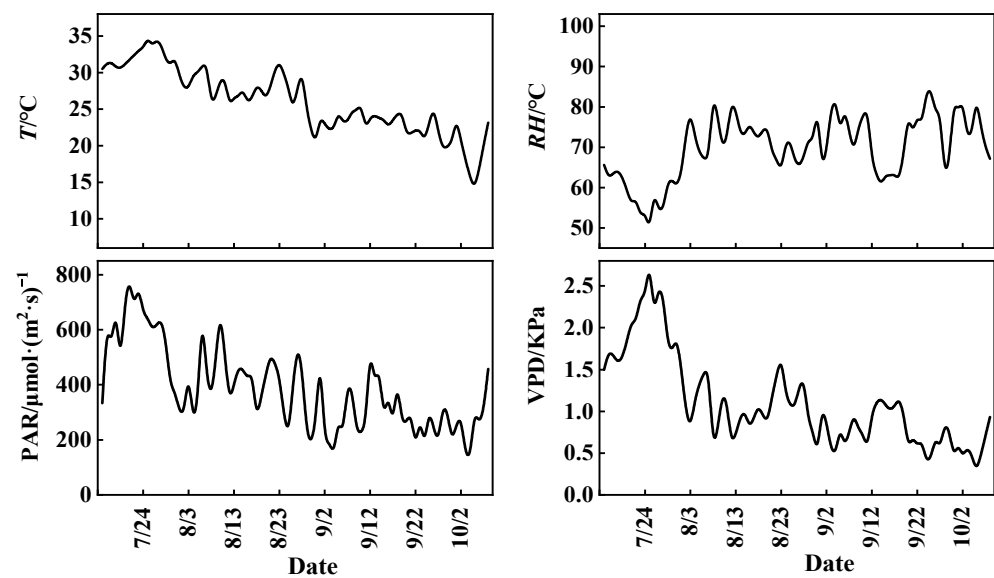


Figure 1. The daily variations in meteorological factors during the rice growing season.

Figure 2 illustrates the diurnal variations in CO_2 concentration during the rice growing season. The overall pattern of CO_2 concentration shows a distinct “peak-trough” pattern, with lower levels during the day and higher levels at night, similar to the observations of previous studies [16]. From sunrise, as atmospheric turbulence and rice photosynthetic activity intensify, the CO_2 concentration in the atmosphere begins to decrease rapidly, reaching its minimum around 16:00. This is attributed to the unstable boundary layer in the afternoon, which enhances turbulent exchange, facilitating the diffusion of CO_2 . Meanwhile, the strong photosynthetic activity of rice in the afternoon absorbs a considerable amount of CO_2 [17]. Subsequently, due to the weakening of rice photosynthesis and convective transport (i.e., reduced CO_2 sink strength), CO_2 released from soil and biological respiration, industrial production, etc., gradually accumulates in the atmosphere, leading to an upward trend in concentration until it peaks the following morning.

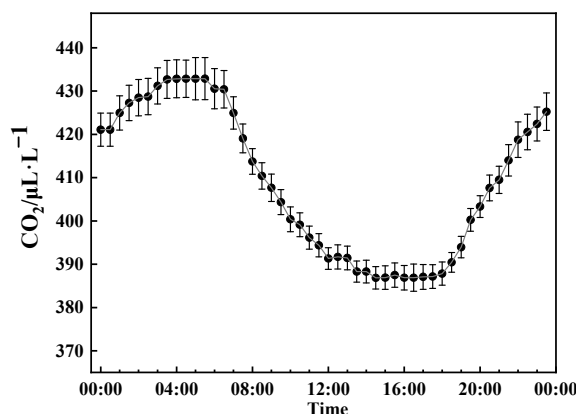


Figure 2. Diurnal variation in CO₂ concentration (mean ± standard error) during the rice growing season.

3.2. The Variation in CO₂ Flux

Figure 3 shows the time series variation in 30 min averaged CO₂ flux during daytime periods throughout the rice growing season. Due to factors such as instrument malfunctions, power outages at the site, and weather conditions, data are missing for the following dates: 24–25 July, 30–31 July, 4–8 August, 10 August, 12 August, 14 August, 3–4 September, 24–25 September, 30 September, 2 October, and 5 October. Data for all other times remain intact. It is important to note that the 30 min CO₂ flux data observed by the eddy covariance system represent the net carbon exchange (NEE) between the terrestrial ecosystem and the atmosphere. Therefore, the CO₂ flux described in this study represented the NEE, indicating the net CO₂ uptake by rice, with negative values indicating downward flux. As shown in the Figure 3, the range of 30 min CO₂ flux throughout the entire rice observation period varies from -0.1 to $-38.4 \mu\text{mol}\cdot(\text{m}^2\cdot\text{s})^{-1}$, with an average of $-12.9 \mu\text{mol}\cdot(\text{m}^2\cdot\text{s})^{-1}$. Combining these results with Figure 4, it can be seen that the CO₂ flux reaches its highest value during the flowering stage of rice. This might be attributed to the peak physiological activity of rice during this stage, characterized by vigorous photosynthesis and greater canopy conductance, resulting in enhanced CO₂ uptake by the rice [18]. Although CO₂ concentration remains relatively high during the later stages of the growing season, the reduced physiological activity of rice at this time leads to a slowdown in CO₂ uptake.

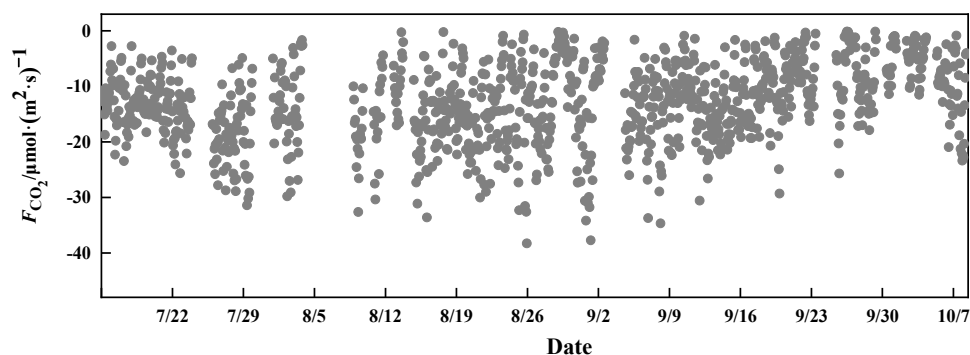


Figure 3. Time series variation in daytime CO₂ flux during the rice growing season.

Since the observed CO₂ flux reflects the exchange of CO₂ between the soil, vegetation, and the atmosphere, namely the remainder after deducting the total ecosystem respiration (R_{eco}) from the gross primary productivity (GPP), the magnitude of CO₂ flux indicates the intensity of this condition. If the intensity of photosynthesis of crop exceeds that of soil/crop respiration, the crop's CO₂ uptake is represented as net absorption, with a negative flux. Conversely, soil/crop releases CO₂ to the atmosphere, with a positive flux.

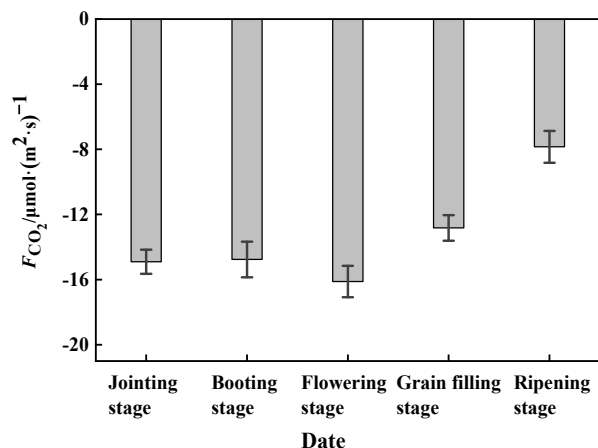


Figure 4. Seasonal variation in daytime CO₂ flux during the rice growing season.

The diurnal variation in CO₂ flux during the rice growing season indicates a U-shaped curve (Figure 5). The nighttime CO₂ flux is positive and relatively stable, indicating that the rice field ecosystem is a source of atmospheric CO₂. The daytime CO₂ flux is negative, indicating that CO₂ uptake is predominant in the rice ecosystem. The flux value of rice changes from positive to negative between 06:30 and 07:00, indicating a transition of the ecosystem from a carbon source to a carbon sink. Subsequently, with the increase in solar radiation intensity, CO₂ flux rapidly increases and reaches its maximum around 11:30, followed by a slow decrease until 12:00, when an abnormal decrease occurs. This is the phenomenon of “midday depression”, which occurs due to intense sunlight and disappears as sunlight diminishes, consistent with earlier observations at the same location [19]. The occurrence of this phenomenon is related to “photoinhibition” occurring after photosynthetically active radiation reaches the light saturation point. This can be explained as follows: CO₂/H₂O flux and canopy conductance increase with the enhancement of photosynthetically active radiation starting from the morning. When the light saturation point of crop leaves is reached, “photoinhibition” occurs, resulting in a decrease in CO₂ absorption flux. Crops respond to strong light by exhibiting physiological reactions such as upper leaf curling and reduction in effective leaf area, leading to a decrease in water vapor flux and canopy conductance [20]. As photosynthetically active radiation gradually decreases, upper leaves unfold, and CO₂/H₂O flux and canopy conductance slowly recover. Subsequently, the variation in CO₂ flux returns to normal. In the afternoon, the decrease in solar radiation leads to a decline in the photosynthetic capacity of rice, resulting in a decreasing trend in CO₂ flux. However, this downward trend does not lead to an increase in CO₂ concentration in the afternoon, which may be mainly attributed to the unstable atmospheric stratification and strong meteorological diffusion conditions in the afternoon [21].

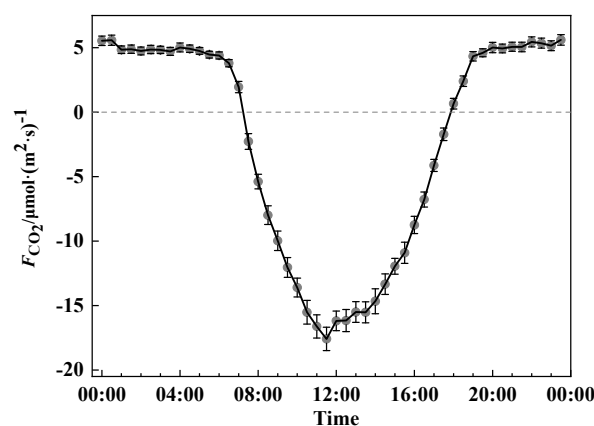


Figure 5. Diurnal variation in CO₂ flux (mean ± standard error) during the rice growing season.

3.3. Parameterization of the CO₂ Flux Model

Figure 6 presents a boundary line analysis of the limiting effects of PAR, T, VPD, Phen, Time, and CO₂ concentration on rice CO₂ flux. This analysis was conducted to determine the parameter values of the limiting functions within the model. The maximum CO₂ flux represents the rice CO₂ flux under the most favorable conditions for all climate and environmental factors throughout the observation period. In this study, the observed maximum CO₂ flux was 38.4 $\mu\text{mol}\cdot(\text{m}^2\cdot\text{s})^{-1}$, slightly lower than the experimental results of Tong et al. in China [14,22]. This discrepancy may be related to crop variety, observation methods, or other factors. The large number of data obtained in this study were collected using the eddy covariance method under non-controlled experimental conditions, resulting in a more abundant sample size and a more scientific observation method compared to other studies. The minimum CO₂ flux was less than 1% of the maximum flux value, so the f_{min} in the model was set to 0.01.

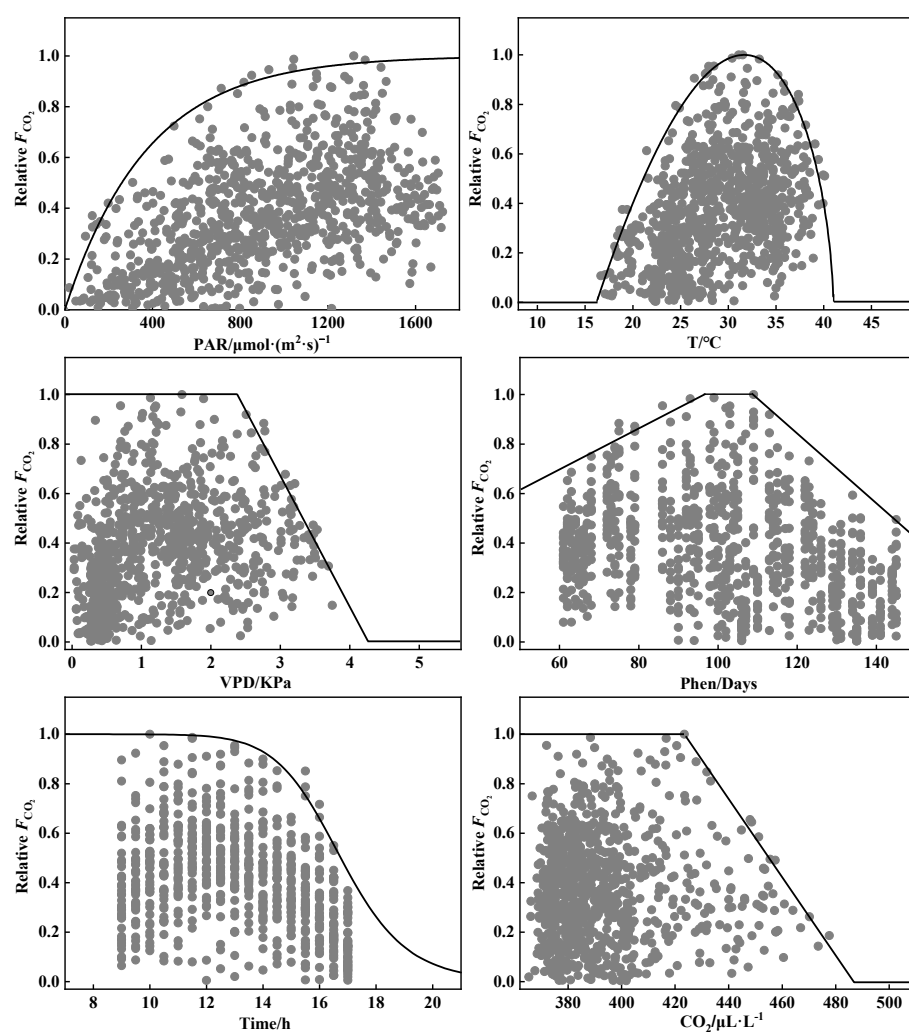


Figure 6. The limiting effects of different climatic factors on rice CO₂ flux.

Light is an important driving factor affecting the opening and closing of rice leaf stomata. It can also affect CO₂ absorption through non-stomatal pathways by altering the rate of surface oxidation reactions in rice, thereby influencing rice canopy CO₂ flux through the combined effects of these two aspects [23,24]. From Figure 6, it can be seen that the CO₂ flux for rice exhibits a clear saturation light response pattern. Under low light conditions, the CO₂ flux is low. As light intensity further increases, the flux gradually increases, with a rapid rate of change. When PAR increases to around 800 $\mu\text{mol}\cdot(\text{m}^2\cdot\text{s})^{-1}$, rice CO₂ flux tends to saturate and is then maintained at its respective maximum level.

T controls the movement of rice leaf stomata by affecting enzyme activity, thereby indirectly affecting rice canopy CO₂ flux. Generally, as T rises, CO₂ absorption flux gradually increases, and when the T exceeds a certain threshold, the flux value will rapidly decrease [25]. Similarly, as seen in Figure 6, rice CO₂ flux exhibits a clear unimodal curve pattern with increasing T, reaching its maximum at 31.6 °C, within a temperature range of 16.2~40.9 °C. When the T exceeds this range, CO₂ flux is nearly zero.

When VPD exceeds 2.38 KPa, CO₂ flux shows a linear downward trend and is suppressed. When VPD exceeds 4.22 KPa, the flux value becomes zero. This phenomenon occurs because lower VPD favors the timely and effective replenishment of water lost by plants while in higher VPD environments, the content of abscisic acid in plants increases significantly, leading to stomatal closure to reduce water transpiration.

Additionally, rice CO₂ flux initially increases linearly, reaching its peak at 99 days after sowing, which is maintained until 109 days after sowing, after which it rapidly decreases linearly. This is consistent with the observations of Tong et al. [14] on rice in southern China. Time also imposes certain limitations on rice CO₂ flux. Flux values are notably higher and relatively stable in the morning, gradually decreasing rapidly after noon, and eventually approaching zero.

Rice CO₂ flux is also influenced by its concentration. The concentration of CO₂ in rice will affect its photosynthetic rate, thereby influencing the flux of CO₂. Therefore, if rice is grown in an environment with a high CO₂ concentration, its photosynthesis will be more efficient, resulting in an increase in CO₂ flux [16]. However, it is important to note that the effect of CO₂ concentration on photosynthesis is not linear but is influenced by other factors such as light intensity, temperature, etc. With increasing concentration, rice CO₂ flux is maintained at a relatively high level (Figure 6). When CO₂ concentration exceeds 423.4 μL·L⁻¹, the flux value rapidly decreases linearly.

3.4. Validation of the CO₂ Flux Model

Based on the boundary analysis of the relationship between rice CO₂ flux and various environmental factors mentioned above, the parameter values applicable to the flux model were obtained, as shown in Table 1. By substituting the parameter values with observed climatic environmental variables into each stress coefficient, the characteristics of changes in f_{temp} , f_{VPD} , f_{PAR} , f_{phen} , f_{Time} , and f_{CO_2} can be calculated. Then, according to the Jarvis multiplication model, rice CO₂ flux can be simulated.

Table 1. Parameter values of stress coefficient in rice CO₂ flux model.

Stress Coefficient	Parameter	Unit	Parameter Value	
			Before Revision	After Revision
$F_{CO_2,max}$	—	μmol·(m ² ·s) ⁻¹	41.4	38.4
f_{min}	—	—	0.01	0.01
f_{PAR}	L	—	0.0026	0.0027
f_{temp}	t_{min}	°C	20.2	16.2
	t_{opt}	°C	31.6	31.7
	t_{max}	°C	40.5	40.9
f_{VPD}	VPD_{max}	KPa	1.8	2.38
	VPD_{min}	KPa	3.0	4.22
	Day_c	D	93	99
	Day_d	D	102	109
f_{phen}	c_1	—	0.0043	0.0084
	d_1	—	0.60	0.20
	c_2	—	-0.022	-0.0143
	d_2	—	3.28	2.54
f_{Time}	e	—	16.6	16.7
	f	—	13.8	14.4
f_{CO_2}	$C_{CO_2,min}$	μL·L ⁻¹	—	486.2
	$C_{CO_2,max}$	μL·L ⁻¹	—	423.4

To compare and validate the applicability of the model, linear regression analysis was conducted to compare the relationship between the measured and simulated values of CO₂ flux, as shown in Figure 7. *t*-test analysis showed that there was no significant difference between the simulated and measured values ($p < 0.001$), with a correlation coefficient R^2 of 0.64 for the regression model, indicating that the revised model explains 64% of the variability in rice CO₂ flux. Meanwhile, when the flux values were low, the simulated results were consistently higher, suggesting the possible presence of other environmental constraints in such cases. Conversely, when the flux values were high, the simulated results were noticeably lower than the actual levels. In addition, the slope of the regression line was 0.81, with an intercept of 4.26, accounting for 11.1% of the maximum flux value, meeting the accuracy requirements.

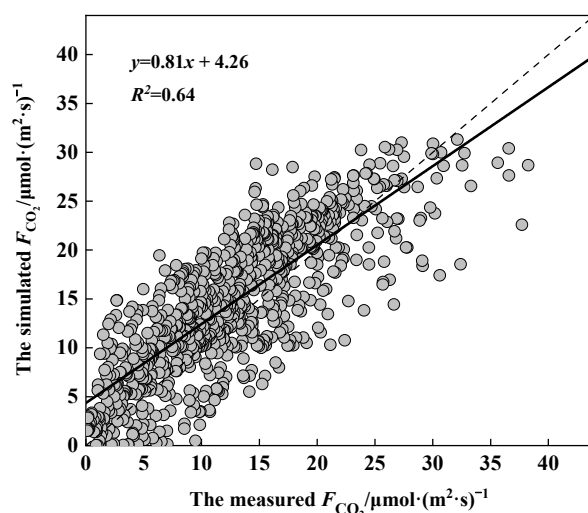


Figure 7. Validation of rice CO₂ flux model.

4. Conclusions

This study found that the variation range of 30 min CO₂ flux in the rice ecosystem was -0.1 to $-38.4 \mu\text{mol}\cdot(\text{m}^2\cdot\text{s})^{-1}$, with an average of $-12.9 \mu\text{mol}\cdot(\text{m}^2\cdot\text{s})^{-1}$. The highest flux values occurred during the flowering stage of rice, during which the photosynthetic capacity of rice was strong and biological activities were vigorous, resulting in a higher net absorption of CO₂. The CO₂ flux during the rice growing season displayed a diurnal pattern characterized by an initial increase followed by a decrease. Moreover, there was a sudden abnormal decrease at around 12:00, which could be attributed to the phenomenon of the crop's midday dormancy. In addition, PAR, T, VPD, Phen, Time, and CO₂ concentration were all important factors influencing the rice canopy CO₂ flux. When PAR exceeded $800 \mu\text{mol}\cdot(\text{m}^2\cdot\text{s})^{-1}$, T was approximately $31.6 \text{ }^\circ\text{C}$, VPD was less than 2.38 KPa , CO₂ concentration was below $423.4 \mu\text{L}\cdot\text{L}^{-1}$, etc., rice CO₂ flux was at a relatively high level. The response pattern of rice canopy CO₂ flux to various environmental factors was similar to that of stomatal conductance to environmental factors, indicating that canopy and leaf activities under the influence of various environmental factors had similar impact mechanisms. The simulated CO₂ flux using the parameterized model was compared with measured values, and it was found that the parameter model established in this study could be used to simulate rice CO₂ flux.

Author Contributions: Conceptualization, J.W. (Jinghan Wang) and J.W. (Jiayan Wang); methodology, H.Z., J.W. (Jinghan Wang) and Y.Z.; formal analysis, H.Z. and J.W. (Jiayan Wang); writing—original draft preparation, H.Z., J.W. (Jinghan Wang), J.W. (Jiayan Wang) and Y.Z.; writing—review and editing, H.Z. and J.W. (Jinghan Wang). All authors have read and agreed to the published version of the manuscript.

Funding: This research was funded by the China Postdoctoral Science Foundation (2020M681157).

Institutional Review Board Statement: Not applicable.

Informed Consent Statement: Not applicable.

Data Availability Statement: The data presented in this study are available on request from the corresponding author. The data are not publicly available due to privacy.

Conflicts of Interest: The authors declare no conflict of interest.

References

1. Fedorov, V.B.; Trucchi, E.; Goropashnaya, A.V.; Waltari, E.; Whidden, S.E.; Stenseth, N.C. Impact of past climate warming on genomic diversity and demographic history of collared lemmings across the Eurasian Arctic. *Proc. Natl. Acad. Sci. USA* **2020**, *117*, 3026–3033. [[CrossRef](#)] [[PubMed](#)]
2. Zickfeld, K.; Eby, M.; Matthews, H.D.; Weaver, A.J. Setting cumulative emissions targets to reduce the risk of dangerous climate change. *Proc. Natl. Acad. Sci. USA* **2009**, *106*, 16129–16134. [[CrossRef](#)] [[PubMed](#)]
3. Fan, J.; McConkey, B.G.; Liang, B.C.; Angers, D.A.; Janzen, H.H.; Kröbel, R.; Cerkowniak, D.D.; Smith, W.N. Increasing crop yields and root input make Canadian farmland a large carbon sink. *Geoderma* **2019**, *336*, 49–58. [[CrossRef](#)]
4. Lei, H.; Yang, D. Seasonal and interannual variations in carbon dioxide exchange over a cropland in the North China Plain. *Glob. Change Biol.* **2010**, *16*, 2944–2957. [[CrossRef](#)]
5. Yue, Y.; Ni, J.; Ciais, P.; Piao, S.; Wang, T.; Huang, M.; Borthwick, A.G.L.; Li, T.; Wang, Y.; Chappell, A.; et al. Lateral transport of soil carbon and land-atmosphere CO₂ flux induced by water erosion in China. *Proc. Natl. Acad. Sci. USA* **2016**, *113*, 6617–6622. [[CrossRef](#)]
6. Wang, J.; Yu, Q.; Li, J.; Li, L.-H.; Li, X.-G.; Yu, G.-R.; Sun, X.-M. Simulation of diurnal variations of CO₂, water and heat fluxes over winter wheat with a model coupled photosynthesis and transpiration. *Agric. For. Meteorol.* **2006**, *137*, 194–219. [[CrossRef](#)]
7. Mei, B.; Zheng, X.; Xie, B.; Dong, H.; Zhou, Z.; Wang, R.; Deng, J.; Cui, F.; Tong, H.; Zhu, J. Nitric oxide emissions from conventional vegetable fields in southeastern China. *Atmos. Environ.* **2009**, *43*, 2762–2769. [[CrossRef](#)]
8. Chen, H.; Li, H.; Wei, Y.; McBean, E.; Liang, H.; Wang, W.; Huang, J.J. Partitioning eddy covariance CO₂ fluxes into ecosystem respiration and gross primary productivity through a new hybrid four sub-deep neural network. *Agric. Ecosyst. Environ.* **2024**, *361*, 108810. [[CrossRef](#)]
9. Baldocchi, D.D. Assessing the eddy covariance technique for evaluating carbon dioxide exchange rates of ecosystems: Past, present and future. *Glob. Change Biol.* **2003**, *9*, 479–492. [[CrossRef](#)]
10. Huang, Y.; Yu, Y.; Zhang, W.; Sun, W.; Liu, S.; Jiang, J.; Wu, J.; Yu, W.; Wang, Y.; Yang, Z. Agro-C: A biogeophysical model for simulating the carbon budget of agroecosystems. *Agric. For. Meteorol.* **2009**, *149*, 106–129. [[CrossRef](#)]
11. Zhao, H.; Huang, J.; Zheng, Y. Observation of ozone deposition flux and its contribution to stomatal uptake over a winter wheat field in eastern China. *Atmos. Environ.* **2024**, *326*, 120472. [[CrossRef](#)]
12. Massman, W.J.; Lee, X. Eddy covariance flux corrections and uncertainties in long-term studies of carbon and energy exchanges. *Agric. For. Meteorol.* **2002**, *113*, 121–144. [[CrossRef](#)]
13. Falge, E.; Baldocchi, D.; Olson, R.; Anthoni, P.; Aubinet, M.; Bernhofer, C.; Burba, G.; Ceulemans, R.; Clement, R.; Dolman, H.; et al. Gap filling strategies for defensible annual sums of net ecosystem exchange. *Agric. For. Meteorol.* **2001**, *107*, 43–69. [[CrossRef](#)]
14. Tong, L.; Wang, X.; Geng, C.; Wang, W.; Lu, F.; Song, W.; Liu, H.; Yin, B.; Sui, L.; Wang, Q. Diurnal and phenological variations of O₃ and CO₂ fluxes of rice canopy exposed to different O₃ concentrations. *Atmos. Environ.* **2011**, *45*, 5621–5631. [[CrossRef](#)]
15. Wu, R.J.; Zheng, Y.F.; Hu, C.D. Evaluation of the chronic effects of ozone on biomass loss of winter wheat based on ozone flux-response relationship with dynamical flux thresholds. *Atmos. Environ.* **2016**, *142*, 93–103. [[CrossRef](#)]
16. Hu, S.; Li, T.; Wang, Y.; Gao, B.; Jing, L.; Zhu, J.; Wang, Y.; Huang, J.; Yang, L. Effects of free air CO₂ enrichment (FACE) on grain yield and quality of hybrid rice. *Field Crops Res.* **2024**, *306*, 109237. [[CrossRef](#)]
17. Bonilla-Cordova, M.; Cruz-Villacorta, L.; Echegaray-Cabrera, I.; Ramos-Fernández, L.; Flores del Pino, L. Design of a Portable Analyzer to Determine the Net Exchange of CO₂ in Rice Field Ecosystems. *Sensors* **2024**, *24*, 402. [[CrossRef](#)] [[PubMed](#)]
18. Demyan, M.S.; Ingwersen, J.; Funkuin, Y.N.; Ali, R.S.; Mirzaeitalarpshiti, R.; Rasche, F.; Poll, C.; Müller, T.; Streck, T.; Kandeler, E.; et al. Partitioning of ecosystem respiration in winter wheat and silage maize—Modeling seasonal temperature effects. *Agric. Ecosyst. Environ.* **2016**, *224*, 131–144. [[CrossRef](#)]
19. Xu, J.; Zheng, Y.; Mai, B.; Zhao, H.; Chu, Z.; Huang, J.; Yuan, Y. Simulating and partitioning ozone flux in winter wheat field: The Surf-atm-O₃ model. *China Environ. Sci.* **2018**, *38*, 455–470. (In Chinese)
20. Murata, N.; Takahashi, S.; Nishiyama, Y.; Allakhverdiev, S.I. Photoinhibition of photosystem II under environmental stress. *Biochim. Biophys. Acta BBA Bioenerg.* **2007**, *1767*, 414–421. [[CrossRef](#)]
21. Pérez, I.A.; Sánchez, M.L.; García M, A.; Pardo, N.; Fernández-Duque, B. The influence of meteorological variables on CO₂ and CH₄ trends recorded at a semi-natural station. *J. Environ. Manag.* **2018**, *209*, 37–45. [[CrossRef](#)] [[PubMed](#)]
22. Tong, L.; Xiao, H.; Qian, F.; Huang, Z.; Feng, J.; Wang, X. Daytime and phenological characteristics of O₃ and CO₂ fluxes of winter wheat canopy under short-term O₃ exposure. *Water Air Soil Pollut.* **2016**, *227*, 1–14. [[CrossRef](#)]
23. Fares, S.; McKay, M.; Holzinger, R.; Goldstein, A.H. Ozone fluxes in a *Pinus ponderosa* ecosystem are dominated by non-stomatal processes: Evidence from long-term continuous measurements. *Agric. For. Meteorol.* **2010**, *150*, 420–430. [[CrossRef](#)]

24. Stella, P.; Personne, E.; Loubet, B.; Lamaud, E.; Ceschia, E.; Béziat, P.; Bonnefond, J.M.; Irvine, M.; Keravec, P.; Mascher, N.; et al. Predicting and partitioning ozone fluxes to maize crops from sowing to harvest: The Surf atm-O₃ model. *Biogeosciences* **2011**, *8*, 2869–2886. [[CrossRef](#)]
25. Zhang, W.; Feng, Z.; Wang, X.; Liu, X.; Hu, E. Quantification of ozone exposure- and stomatal uptake-yield response relationships for soybean in Northeast China. *Sci. Total Environ.* **2017**, *599–600*, 710–720. [[CrossRef](#)]

Disclaimer/Publisher’s Note: The statements, opinions and data contained in all publications are solely those of the individual author(s) and contributor(s) and not of MDPI and/or the editor(s). MDPI and/or the editor(s) disclaim responsibility for any injury to people or property resulting from any ideas, methods, instructions or products referred to in the content.